Extreme Flood Response: The June 2008 Flooding in Iowa

JAMES A. SMITH AND MARY LYNN BAECK

Department of Civil and Environmental Engineering, Princeton University, Princeton, New Jersey

GABRIELE VILLARINI

IIHR—Hydroscience and Engineering, The University of Iowa, Iowa City, Iowa

DANIEL B. WRIGHT

Department of Civil and Environmental Engineering, Princeton University, Princeton, New Jersey

WITOLD KRAJEWSKI

IIHR—Hydroscience and Engineering, The University of Iowa, Iowa City, Iowa

(Manuscript received 20 December 2012, in final form 12 April 2013)

ABSTRACT

The authors examine the hydroclimatology, hydrometeorology, and hydrology of extreme floods through analyses that center on the June 2008 flooding in Iowa. The most striking feature of the June 2008 flooding was the flood peak of the Cedar River at Cedar Rapids ($3964\,m^3\,s^{-1}$), which was almost twice the previous maximum from a record of 110 years. The spatial extent of extreme flooding was exceptional, with more U.S. Geological Survey stream gauging stations reporting record flood peaks than in any other year. The 2008 flooding was produced by a sequence of organized thunderstorm systems over a period of two weeks. The authors examine clustering and seasonality of flooding in the Iowa study region and link these properties to features of the June 2008 flood event. They examine the environment of heavy rainfall in Iowa during June 2008 through analyses of composite rainfall fields (15-min time interval and 1-km spatial resolution) developed with the Hydro-NEXRAD system and simulations using the Weather Research and Forecasting Model (WRF). Water balance analyses of extreme flood response, based on rainfall and discharge observations from basins with extreme flooding, suggest that antecedent soil moisture plays a diminishing role in flood response as the return interval increases. Rainfall structure and evolution play a critical and poorly understood role in determining the scaling of flood response. As in other extreme flood studies, analyses of the Iowa flood data suggest that measurement errors can be significant for record discharge estimates.

1. Introduction

In this paper, we examine the hydroclimatology, hydrometeorology, and hydrology of extreme floods through analyses that center on the June 2008 flooding in Iowa (Fig. 1). The 2008 flooding was produced by a series of storms extending from 29 May through 12 June 2008. The 13 June 2008 flood peak of the Cedar River at Cedar Rapids (drainage area of $16\,861\,km^2$) of $3964\,m^3\,s^{-1}$ was almost twice the previous maximum from a record of 110 years. The spatial extent of flooding in the upper Midwest was also unprecedented, with more record flood peaks at U.S. Geological Survey (USGS) stream gauging stations in Iowa than for any other flood (section 3a).

The main objectives of this study are to characterize the hydrometeorological and hydrologic processes responsible for the June 2008 flooding in Iowa, with special attention to the exceptional flood peak of the Cedar River at Cedar Rapids, and to place the June 2008 flood in a hydroclimatological context. Discharge observations from USGS stream gauging stations in Iowa provide a key resource for examining the hydrology of extreme flooding. We use long USGS stream gauging records in Iowa (see section 2) to examine the hydroclimatology of

Corresponding author address: James A. Smith, Department of Civil and Environmental Engineering, Princeton University, Engineering Quadrangle, Princeton, NJ 08540.
E-mail: jsmith@princeton.edu

DOI: 10.1175/JHM-D-12-0191.1

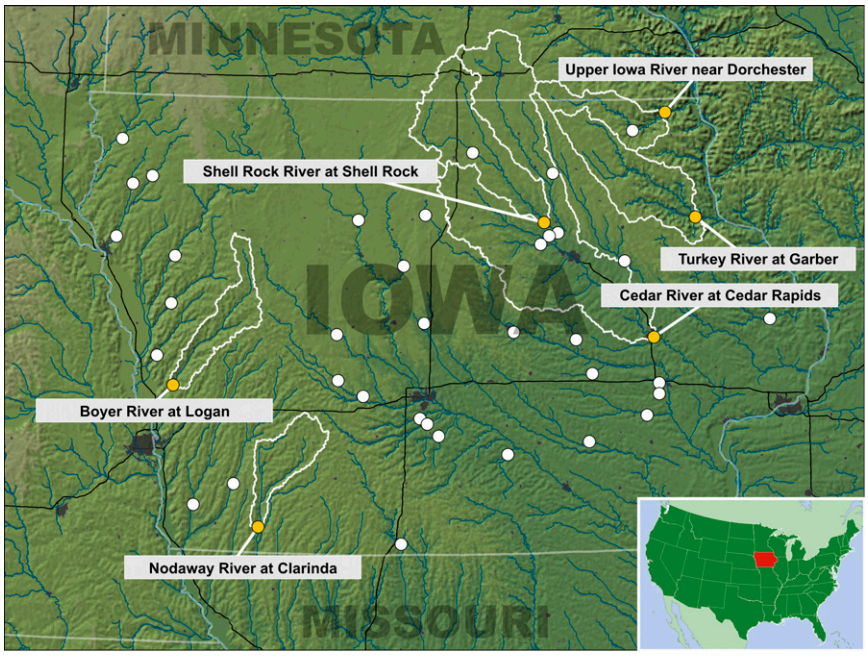

FIG. 1. Iowa study area. Basin boundaries for the Boyer, Nodaway, Shell Rock, Cedar River (Cedar Rapids), Upper Iowa, and Turkey River are shown. Colored circles indicate USGS stream gauging locations used for hydroclimatological analyses.

flooding in the region and to relate these analyses to properties of the June 2008 flooding. We use composite rainfall fields for the Iowa region developed from the Hydro-NEXRAD system (Seo et al. 2010; Krajewski et al. 2010b) at 15-min time resolution and 1-km horizontal resolution for hydrometeorological and hydrologic analyses. Storm tracking algorithms (Dixon and Wiener 1993) are used to examine storm evolution for thunderstorm systems that produced extreme flooding during the June 2008 period. We also use simulations based on the Weather Research and Forecasting Model (WRF) to examine elements of the atmospheric environment that controlled rainfall distribution for the June 2008 storm systems.

Analyses of the June 2008 flooding in Iowa are designed to illustrate key features of extreme flooding in regions for which warm season thunderstorm systems are major flood agents. An important class of questions addressed in this study concerns the relationships between physical processes that control the ''upper tail'' of flood peak magnitudes and physical processes that control more common floods (see, e.g., Smith 1987, 1989; Villarini and Smith 2010). The June 2008 flooding in Iowa provides a setting in which exceptional observations are available (see section 2) for examining hydrometeorological and hydrologic processes for a very rare flood event (see section 3 for quantitative analyses of how rare the flooding was). The specific questions that motivate the study are the following: 1) How extreme was the June 2008 Iowa flooding?; 2) What was the role of ''clustering'' for flood processes during the June 2008 flood and how do June 2008 flood and storm occurrences compare with hydroclimatological features of flood and storm occurrences?; 3) Were severe thunderstorms important flood agents for the June 2008 storms?; 4) What was the role of land surface processes in controlling the spatial and temporal distribution of extreme rainfall over Iowa during the June 2008 flood period?; 5) Was antecedent soil moisture an important element of extreme flood response for the June 2008 flooding?; and 6) What were scaling properties of flood peaks for the June 2008 flood and how do they compare with other major flood events in the Iowa study region?

The hydroclimatology of flooding in Iowa is characterized by seasonal maxima of flood occurrences in the April–June time period (Villarini et al. 2011a,b; Wang and Chen 2009; Schumacher and Johnson 2006) and by the occurrence of multiple floods during major flood years like 1993 and 2008 (Budikova et al. 2010; Coleman and Budikova 2010; Villarini et al. 2013). Links between climate variability and extremes of the hydrologic cycle in Iowa have been examined in previous studies (Changnon and Kunkel 1995; Guetter and Georgakakos 1996; Kunkel et al. 1994; Budikova et al. 2010; Villarini et al. 2013).

The storm systems that produced flooding in Iowa from 29 May through 12 June 2008 were mesoscale convective

systems (MCSs). The spatial structure and temporal evolution of flood-producing rainfall from MCSs have been summarized by Schumacher and Johnson (2005). The storm systems that affected Iowa during the 29 May to 12 June time period also produced damaging hail, copious lightning, and multiple tornados (see section 3b). The role of severe thunderstorm systems as flood agents has not been fully established, with some studies suggesting that severe thunderstorms are poor candidates for producing floods because of the relatively low precipitation efficiency of the storms (Cotton and Anthes 1989), while other studies point to a major role for severe thunderstorm systems in the flood climatology of the United States (Doswell et al. 1996; Smith et al. 2001). The role of land surface processes has received considerable attention in connection with rainfall distribution in the central United States (Trier et al. 2008; Paegle et al. 1996; Dirmeyer and Brubaker 1999; LeMone et al. 2008; DeAngelis et al. 2010; Kustu et al. 2011).

The hydrologic controls of extreme flooding are associated with the spatial and temporal distribution of rainfall, runoff production, and drainage network response. Previous studies have shown that soil moisture in Iowa peaks in June, suggesting that flood response may be dependent on antecedent moisture conditions (Georgakakos and Bae 1994). In Wood et al. (1990), it is suggested that the importance of antecedent moisture decreases with storm total rainfall accumulation, implying that antecedent soil moisture plays a decreasing role in flood response as the return interval becomes more extreme. Storm total rainfall is closely tied to storm structure and evolution. The role of changing agricultural practices, including changes to tillage practices and introduction of tile drains (Potter 1991; Schilling and Libra 2003; Schilling et al. 2008), has been examined as an important source of nonstationarities in flood records in Iowa. The role of rainfall spatial structure for scale-dependent flood response has been examined in previous studies [see, e.g., Robinson et al. 1995; Woods and Sivapalan 1999; Saco and Kumar 2002; Smith et al. 2002; Borga et al. 2007; Merz and Blöschl 2003; Smith et al. 2005; Morin et al. 2006; Viglione et al. 2010). The role of drainage network structure as a key element of scale-dependent flood response is examined in Gupta et al. (2010) through analyses of June 2008 flood peaks in Iowa.

2. Data and methods

Discharge data from USGS stream gauging stations play a central role in this study [see Villarini and Smith (2010) for additional details on USGS stream gauging data]. Analyses utilize instantaneous discharge data, annual peak data, and mean daily discharge data for Iowa. Annual peak observations for 41 stations with records of more than 50 years (Fig. 1) are used to examine the hydroclimatology of flooding and to characterize spatial properties of the June 2008 flooding. The 41 stations are largely nonnested and cover the state of Iowa. Instantaneous discharge data are used from multiple stream gauging stations to examine the hydrology of the June 2008 flooding. Mean daily discharge observations are converted to peaks-over-threshold flood data for two stations, the Shell Rock River and the Nodaway River (see Fig. 1), and are used to examine clustering of flood occurrences (additional details are presented in section 3a).

Radar rainfall fields are derived from volume scan reflectivity observations for multiple radars covering Iowa. The Hydro-NEXRAD processing system converts three-dimensional volume scan reflectivity fields in a polar coordinate system to two-dimensional surface rainfall fields in a Cartesian coordinate system; the time interval between volume scans is approximately 5–6 min. We utilize merging algorithms to compute rainfall from multiple radars (Seo et al. 2010; Krajewski et al. 2010b). Quality control algorithms used for the May–June 2008 rainfall fields include detection and removal of ''anomalous propagation'' (AP) returns (Steiner and Smith 2002) and hail detection and mitigation (Fulton et al. 1998; Baeck and Smith 1998). Conversion of reflectivity to rainfall rate is based on the default National Weather Service Z–R relationship: $R = aZ^b$, where R is rain rate ($\mathrm{mm\,h^{-1}}$), Z is radar reflectivity factor ($\mathrm{mm^6\,m^{-3}}$), and the Z–R parameters take the values $a = 0.017$ and $b = 0.714$ (Fulton et al. 1998). The rainfall accumulation algorithm converts rainfall rate fields on irregular volume scan times (5–6-min time interval) to a regular 15-min time interval [see Villarini et al. (2008) and Krajewski et al. (2010a) for discussion of error characteristics]. The rainfall mapping algorithm converts rainfall fields from a 2D polar coordinate system to the Super–Hydrologic Rainfall Analysis Project (HRAP) coordinate system, a Cartesian coordinate system with horizontal resolution of approximately 1 km (Reed and Maidment 1999).

The Advanced Research version of the WRF (Skamarock et al. 2007) was used for hydrometeorological analyses of the June 2008 storms. We use WRF simulations as a downscaling tool to assess moisture flux over the Iowa study region. The National Centers for Environmental Prediction (NCEP) Eta Model analysis fields are used for initial and boundary conditions (see Ntelekos et al. 2008 for additional details). We also carry out numerical experiments with WRF to examine the role of land surface processes in determining the spatial structure of heavy rainfall over Iowa. In our simulations,

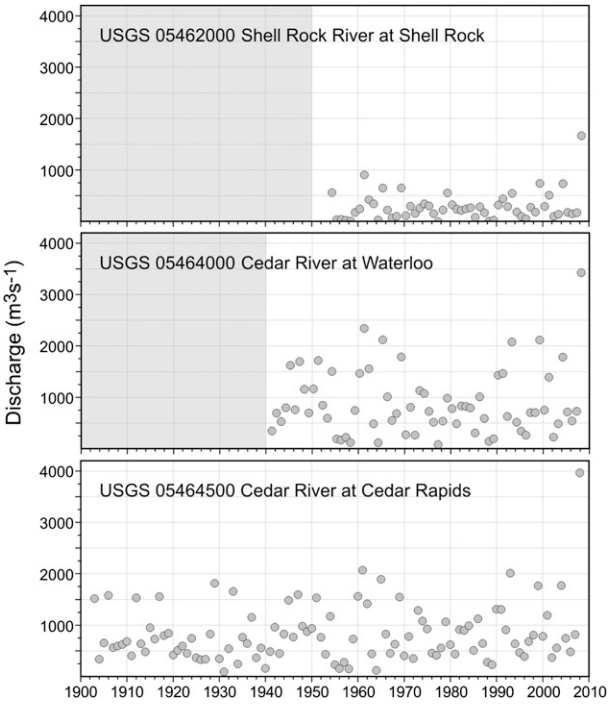

FIG. 2. Annual flood peak time series for (top) Shell Rock, (middle) Cedar River at Waterloo, and (bottom) Cedar River at Cedar Rapids. See Fig. 1 for basin locations (orange circles).

a two-domain nesting configuration is used and results are presented for the inner domain, which has a horizontal resolution of 3 km. Model physics options include 1) the Noah land surface model, 2) the Lin et al. microphysics scheme (Skamarock et al. 2007), 3) the Mellor–Yamada–Janjić planetary boundary layer scheme, 4) the Goddard shortwave radiation scheme, and 5) the Rapid Radiative Transfer Model (RRTM) scheme for longwave radiation [see Ntelekos et al. (2008), Lin et al. (2010), and Smith et al. (2011) for similar case study analyses in the eastern United States]. Cumulus parameterization was not used for either domain (Skamarock et al. 2007), and data assimilation was not used in model simulations.

3. Results

a. Hydroclimatology

In this section, we introduce key elements of the June 2008 flood episode and examine the hydroclimatology of flooding in the Iowa study region from the perspective of these features. Central issues include frequency of extreme flood magnitudes, seasonality and temporal clustering of flood occurrences, and spatial extremes of flood peak magnitudes. These issues are linked to the hydrometeorology of flooding in section 3b and to the hydrology of extreme flooding in section 3c.

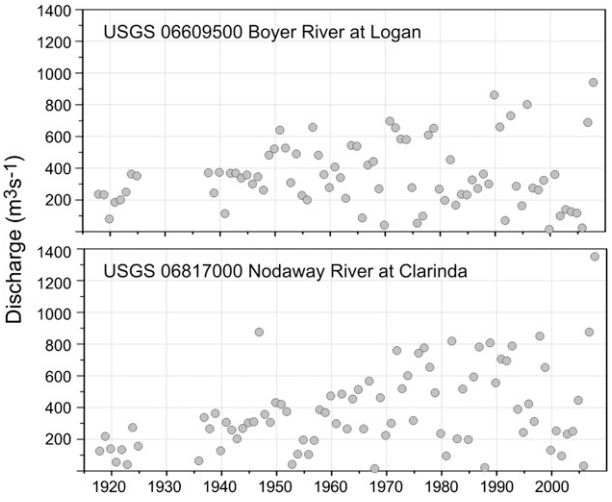

FIG. 3. As in Fig. 2 but for the (top) Boyer River and (bottom) Nodaway River.

The most extreme damage from the June 2008 flooding occurred on the Cedar River at Cedar Rapids (Fig. 1). Annual flood peaks for three stations in the Cedar River basin (Shell Rock River, Cedar River at Waterloo, and Cedar River at Cedar Rapids; Fig. 2) and two stations in western Iowa (Nodaway River and Boyer River; Fig. 3) highlight the extreme magnitudes of the June 2008 flooding (see Fig. 1 for basin and station locations). The June 2008 peak at Cedar Rapids was 1.9 times larger than the second-largest peak from a record of 110 years. The June 2008 peak for the Shell Rock River (drainage area of 4522 km^2) was 1.8 times larger than the second-largest peak from a record of 56 years, and the peak at the Cedar River Waterloo (drainage area of 13 328 km^2) was 1.5 times larger than the second-largest peak from a record of 69 years.

Return intervals of the 2008 flood peaks in the areas of most extreme flooding are long. We estimated return intervals of flood peaks using the generalized extreme value (GEV) distribution and maximum likelihood estimates of model parameters (see Coles 2001). The quantile function (i.e., the inverse of the cumulative distribution function) of the GEV takes the form

$$Q(p) = \alpha - \frac{\beta}{k}\{1 - [-\ln(p)]^{-k}\}, \qquad (1)$$

where $\alpha \in (-\infty, +\infty)$ is the location parameter, $\beta \in (0, +\infty)$ is the scale parameter, and $k \in (-\infty, +\infty)$ is the shape parameter. For $k > 0$, the distribution is unbounded above. For $k < 0$, the distribution is bounded above with an upper bound of $\alpha - (\beta/k)$. Maximum likelihood estimators of the GEV parameters provide the 100-yr flood magnitude through the quantile function evaluated at $p = 0.99$.

Using the entire record for the Cedar River at Cedar Rapids, the estimated 100-yr flood peak is $2956\,m^3\,s^{-1}$, implying that the June 2008 flood peak ($3964\,m^3\,s^{-1}$) is 1.3 times the 100-yr flood magnitude. The estimated return interval for the $3964\,m^3\,s^{-1}$ peak at Cedar Rapids is 340 yr. If the June 2008 flood peak is omitted, the 100-yr flood peak decreases to $2520\,m^3\,s^{-1}$ and the return interval of the June 2008 flood peak increases to 1200 years. The results for the Shell Rock River are comparable, with return intervals of 135 years if 2008 flood is included and 520 years if it is excluded.

The 5 June 2008 peak in the Nodaway River (Fig. 3), which is located in western Iowa (Fig. 1), was 1.5 times larger than the second-largest peak from a record of 91 years and the 8 June 2008 peak in the Boyer was 1.1 times the second-largest peak from a record of 80 years. The Nodaway and Boyer Rivers are located in largely agricultural watersheds and in both drainage basins there have been significant changes in the flood peak distributions (Fig. 3; see also Villarini et al. 2011a for additional analyses). The return interval of the June 2008 peak in the Nodaway is 141 years if the record is restricted to 1970–2009. For the Boyer River the return interval of the 2008 peak is 23 years if the record is restricted to 1970–2009.

Extreme flooding during June 2008 was spatially extensive over the Iowa study region. The 2008 flooding produced record flood peaks at 10 of the 41 stations with long records (locations shown in Fig. 1). The second-largest value was five record flood peaks from 1993. The year 1990 was the only other year with more than two stations with record flood peaks. Another measure of the spatial extent of flooding is the percentage of stations with annual peaks exceeding the 10-yr flood. By this measure, 1993 ranks first with slightly more than 70% of the 41 stations exceeding the 10-yr magnitude. The year 2008 is second with slightly less than 70% of the 41 stations exceeding the 10-yr magnitude. The year 1990 is the only other year with more than 30% of stations exceeding the 10-yr flood magnitude for the station. The spatial extent of extreme flooding is closely linked to scaling properties of flood peak magnitudes (see section 3c for additional discussion).

The late May to early June period of flooding in 2008 matches the climatology of flooding in Iowa well (Villarini et al. 2011a; see also Schumacher and Johnson 2006; Villarini et al. 2011b, 2013). There is a pronounced seasonal peak in flood occurrence during the April–June period (Fig. 4) for the Iowa study region. In Fig. 4, we show the seasonal distribution of flood occurrence and magnitudes for the Nodaway and Shell Rock Rivers. The seasonal peak in flood frequency in the Nodaway, which is located in southwestern Iowa (Fig. 1), occurs in early June, roughly one month later than the seasonal peak in the Shell Rock basin in northeastern Iowa. There are large spatial gradients in the time of maximum flooding in the upper Midwest. In Fig. 5, we illustrate the counts of the 10 largest annual flood peaks at USGS stations that occur during the May–July period (comparable observing periods are used for all stations). Iowa is located in a corridor of high frequency of May–July flood occurrences extending from the Front Range through Nebraska into Iowa. This feature is similar in spatial structure to the climatological maximum of rainfall from mesoscale convective complexes (MCCs; see McAnelly and Cotton 1989; Tuttle and Davis 2006; Zhang et al. 2001). The links between the climatology of MCSs (including MCCs) and flooding warrant additional study.

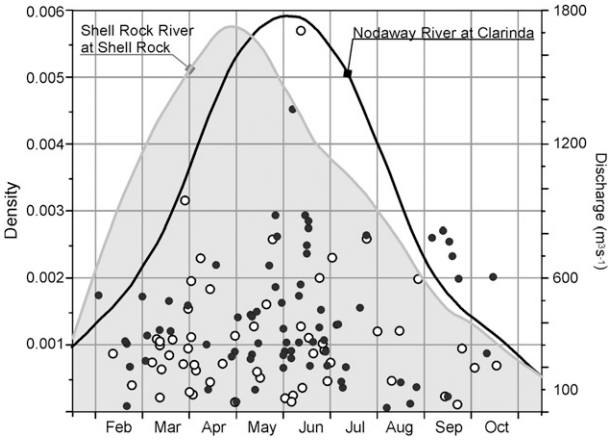

FIG. 4. Time of occurrence (1 = 1 January; 365 = 31 December) during the year for annual flood peaks in the Nodaway (black) and Shell Rock Rivers (white). Sample probability density functions (gray line for Shell Rock and black line for Nodaway) are estimated using a nonparametric estimator.

Flooding over the Iowa study region was the product of a sequence of rain events from 29 May through 12 June (Fig. 6). For the Nodaway River (Fig. 6, top), there were four events (30 May, 5–6 June, 8–9 June, and 12–13 June) with flood peaks larger than $300\,m^3\,s^{-1}$ and three with flood peaks greater than $500\,m^3\,s^{-1}$ (see Fig. 6, top). The storms responsible for peak flooding in the Nodaway during the 5–6 June time period are illustrated in Fig. 7 (see next section for additional discussion of storm properties). During the period of record for the Nodaway gauging station, which has a drainage area of $1970\,km^2$, only 25% of annual peaks exceed $500\,m^3\,s^{-1}$. The record flood peak in the Nodaway River occurred on 6 June 2008 in response to the 5–6 June rain period. For the Shell Rock River (Fig. 6, bottom), as for much of the Cedar River, there were rain events on 30 May, 4–6 June, and 12–13 June, but the extreme flooding in the Shell Rock was principally due to the 7–9 June rain period.

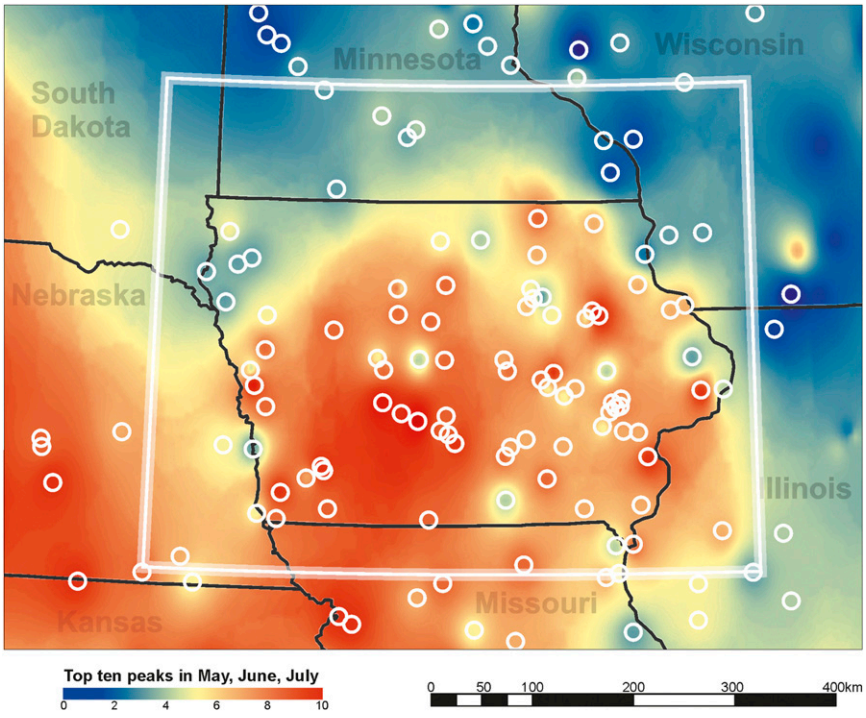

FIG. 5. Count of the top 10 annual flood peaks that occur during May–July. Circles show locations of USGS stations at which we compute the counts of flood peaks during the May–July period.

The role of clustering of storm events in the flood hydroclimatology of Iowa was examined through analyses of peaks-over-threshold flood occurrences for the Nodaway River for 75 years and Shell Rock River for 60 years (figure not shown). The threshold was selected to provide two events per year on average ($126\,m^3\,s^{-1}$ for Nodaway and $150\,m^3\,s^{-1}$ for Shell Rock), with the restriction that events must be separated by 7 days. For the Nodaway River, 21% of years have no peaks and the maximum year (1993) has 11 events. For the Shell Rock River, 28% of years have no peaks and the maximum year (also 1993) has 9 events. The index of dispersion of annual flood counts is 1.8 for the Nodaway and 2.1 for Shell Rock, suggesting that clustering may be a significant component of the flood occurrence process. The index of dispersion (i.e., the ratio of the variance to the mean) takes the value 1.0 for Poisson counts, with values larger than 1.0 indicating overdispersion and values less than 1.0 indicating underdispersion. Clustering of flood occurrences may be due to persistence of atmospheric processes or to land surface processes associated with soil moisture (see Guetter and Georgakakos 1996; Coleman and Budikova 2010; Villarini et al. 2013). Analyses in Villarini et al. (2013), based on the Cox regression model (see Smith and Karr 1986), point to both atmospheric processes and land surface processes (linked to soil moisture) as important elements of clustering of flood occurrences in Iowa. In sections 3b and 3c, we examine hydrometeorological and hydrologic processes for the June 2008 flood that may link clustering to the occurrence of extreme floods.

b. *Hydrometeorology*

Extreme rainfall accumulations were observed from southwestern Iowa to northeastern Iowa (Fig. 8) during the period from 4 to 12 June 2008. We computed storm total accumulations for the 9-day period from 15-min rainfall accumulation fields derived from merged volume scan reflectivity observations for the Des Moines (KDMX), La Crosse (KARX), Omaha (KOAX), Davenport (KDVN), and St. Louis (KLSX) Weather Surveillance Radar-1988 Doppler (WSR-88D) radars using the Hydro-NEXRAD algorithms (see section 2). Accumulations exceeding 400 mm were concentrated near the Nodaway River in southwestern Iowa and the upper Cedar River in northeastern Iowa. The 4–12 June rainfall was principally responsible for record flood peaks in the region. Rainfall accumulations exceeding 200 mm covered a broad region (Fig. 8), with maximum accumulations extending from southwest to northeast through the state. Rainfall accumulations in the northwestern and southeastern corners of the state were less than 50 mm.

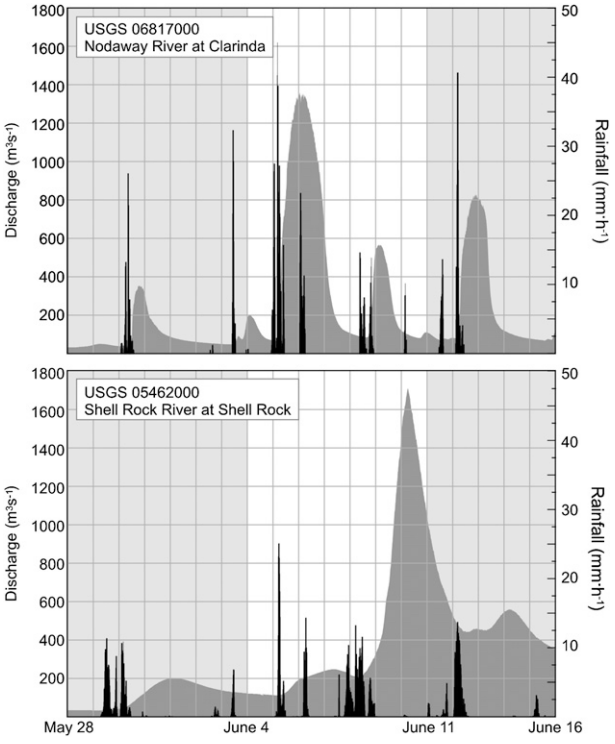

FIG. 6. Time series of basin-averaged rainfall rate (mm h^{-1}, based on 15-min Hydro-NEXRAD rainfall fields) and discharge for the (top) Nodaway and (bottom) Shell Rock River during the period 28 May to 16 June 2008.

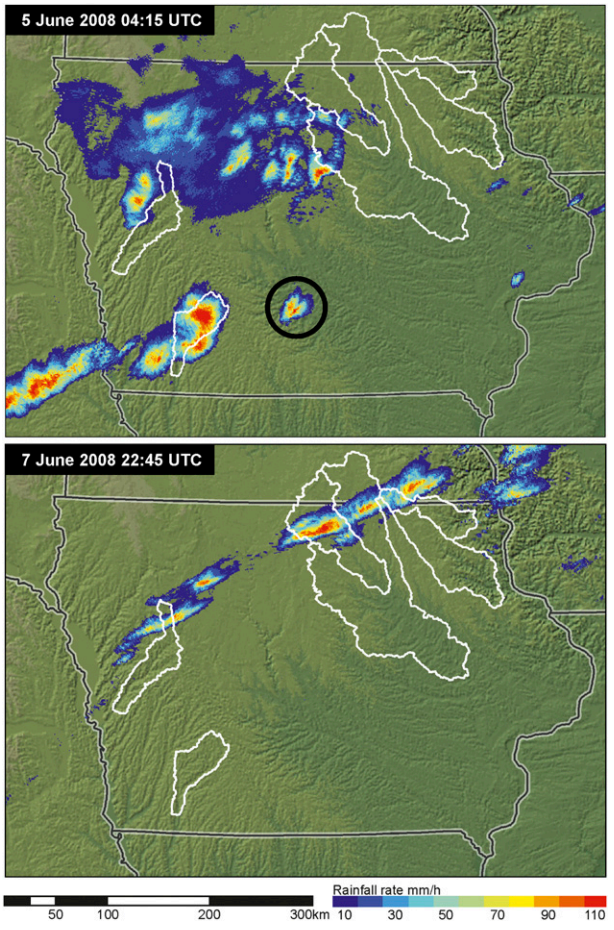

FIG. 7. Rainfall rate fields (15-min time interval) at (top) 0415 UTC 5 June and (bottom) 2245 UTC 7 June 2008. The supercell thunderstorm used for storm tracking analyses is circled in the top panel.

Heavy rainfall during the 4–12 June 2008 period (Fig. 9) was concentrated into major rainfall episodes from 1200 UTC 4 June through 1200 UTC 6 June and from 1200 UTC 7 June through 1200 UTC 9 June. Multiday sequences of heavy rainfall, which have been examined by Tuttle and Davis (2006) and Carbone and Tuttle (2008), reflect atmospheric processes on short time scales that can promote clustering of flood occurrences (see discussion of flood clustering in the preceding section).

The heavy rainfall periods in Iowa were preceded by periods of strong moisture convergence for the study region (Fig. 9). Moisture convergence is defined as the convergence of the vertically integrated water vapor flux vector, that is, the product of specific humidity and the horizontal wind (Rasmusson 1967). We derived the regional rainfall time series averaged over the region (Fig. 9) from 15-min rainfall accumulation fields over the domain illustrated in Fig. 8. Moisture convergence is computed for the same region using model fields derived from WRF simulations (described in section 2). We also computed mean latent heat flux time series from the WRF simulations. Latent heat flux (figure not shown) is small compared with moisture convergence during major rain periods. Extended periods of strong water vapor flux convergence controlled by enhanced synoptic-scale moisture transport associated with westward position of the Bermuda high (figure not shown) played a central role in heavy rainfall production during the 4–12 June period. Heavy rainfall on 8 June was organized along a frontal boundary in the region of elevated low-level moisture transport. The combination of strong humidity transport and large-scale support for vertical motion along the baroclinic zone are key elements of extreme rainfall responsible for the June 2008 flooding in the Cedar River and adjacent basins in northeastern Iowa.

Record flooding in southwestern Iowa, including the Nodaway River basin, was associated with organized thunderstorm systems over the diurnal cycles of 4–5 June and 5–6 June (Fig. 10). Time series of fractional coverage of rainfall greater than 1 mm h^{-1} and 25 mm h^{-1} for the periods 1200 UTC 4 June to 1200 UTC 6 June (Fig. 10) illustrate the cycle of heavy rainfall (peaking

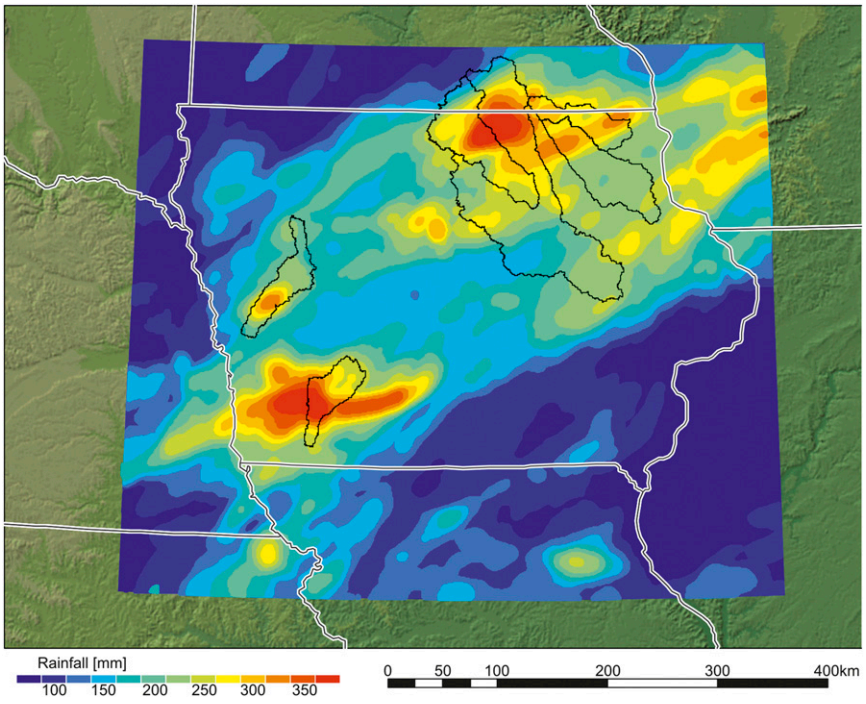

FIG. 8. Total rainfall (mm) from 4 to 12 June 2008 based on Hydro-NEXRAD rainfall fields (see text for details on rainfall analyses).

from 0300 to 0600 UTC on 5 June; see 25 mm h^{-1} results) and the associated development of extensive regional rainfall (see 1 mm h^{-1} results). Similarly, heavy rainfall over the diurnal cycles of 7–8 June and 8–9 June 2008 (Fig. 10) are key to the catastrophic flooding in eastern Iowa.

The storms responsible for record flooding in the Nodaway River (Fig. 7) were severe thunderstorm systems, including multiple supercell thunderstorms, that produced damaging winds, hail, and tornados. The 15-min rainfall field for 5 June (Fig. 7, top) at 0415 UTC illustrates the sequence of storms that passed over the Nodaway River. The storm to the east of the Nodaway basin (circled in Fig. 7) was a supercell thunderstorm that produced multiple tornados and extreme rainfall rates. This storm had passed over the Nodaway River basin, producing heavy rainfall that contributed to the record flood peak of the Nodaway. Storm tracking analyses (Fig. 11) show that maximum reflectivity of the storm remained above 65 dBZ for more than 3 h, with peak reflectivity values of 73 dBZ. During this period the 45-dBZ echo tops exceeded 16 km. Storm area increased steadily to a maximum of more than 1000 km^2. These observations support the hypothesis (see Smith et al. 2001; Doswell et al. 1996) that supercell thunderstorms can play an important role in determining the upper tail of flood peak distributions.

The storm systems producing catastrophic flooding in eastern Iowa during the 7–9 June period (Fig. 7, bottom) were also severe thunderstorm systems. The 15-min rainfall rate field for 2245 UTC on 7 June illustrates storm structure during a period of extreme rainfall over the Shell Rock River basin in the upper Cedar River

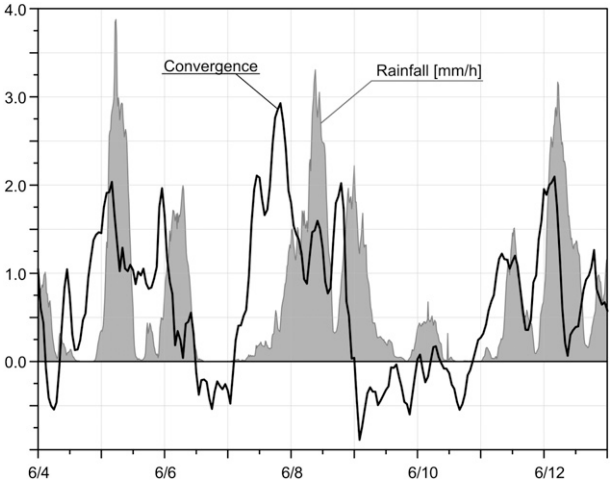

FIG. 9. Time series of regional rainfall (mm h^{-1}) and moisture convergence (mm h^{-1}) for the Iowa study region (Fig. 8). Rainfall time series are derived from Hydro-NEXRAD rainfall fields. Moisture convergence time series are derived from downscaled WRF simulation (see text for details).

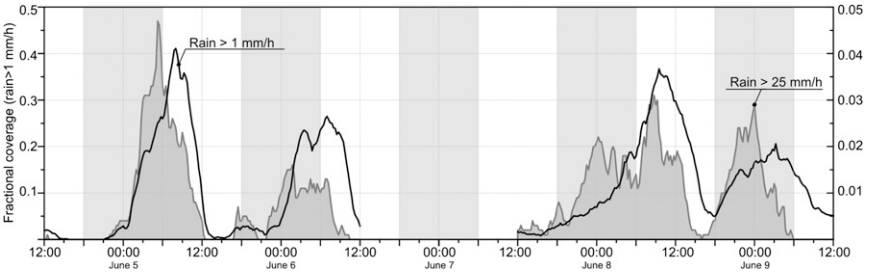

FIG. 10. Fractional coverage of the area with rainfall rates exceeding 25 mm h^{-1} (gray line; right axis with a range from 0.00 to 0.05) and 1 mm h^{-1} (black line; left axis with a range from 0.00 to 0.50) during the period 1200 UTC 4 June to 1200 UTC 9 June for the Iowa study domain (Fig. 8).

watershed. These storms were important elements of heavy rainfall resulting in the record flood peak in the Shell Rock basin (Fig. 6). Severe weather reports included multiple tornados and numerous hail reports (National Climatic Data Center [NCDC] *Storm Reports*).

We performed numerical experiments with WRF (see section 2) to examine the role of land surface processes for storm evolution and rainfall distribution. Analyses are based on two end-member representations of coupling between the land surface and the atmosphere (see LeMone et al. 2008). The Zilintinkevich C relates the roughness length for momentum z_m to the roughness length for heat z_h:

$$z_h = z_m \exp\left[-kC\left(\frac{u_* z_m}{\eta}\right)^{1/2}\right], \qquad (2)$$

where u_* is the friction velocity, k is the von Kármán constant (0.4), η is the kinematic molecular viscosity of air (approximately 1.6 10^{-5} $m^2 s^{-1}$), and C is the Zilintinkevich coefficient. In Fig. 12, we show the rainfall difference field over the Iowa domain for 7–8 June based on simulations with $C = 0.1$ (weak coupling) and $C = 0.5$ (strong coupling). Heavy rainfall is shifted spatially, but both simulations contain comparable rainfall maxima. Rainfall difference fields for the two simulations range from approximately −30 to 30 mm over most of Iowa, with somewhat larger values in the northeastern portion of the study region. These results suggest that land surface processes can alter ''details'' of the heavy rainfall distribution, but not the occurrence of heavy rainfall and flooding over the region. There are differences in the fields of convective available potential energy (CAPE; figures not shown), but in both cases there is an extensive region of extreme CAPE values (greater than 2000 J kg^{-1}) over Iowa. There are pronounced contrasts in latent and sensible heat fluxes between the weak and strong coupling scenarios, but they do not alter the key features of the heavy rain event. Large-scale dynamics, especially in settings with strong moisture convergence, can result in land surface processes playing a secondary role in determining flood properties.

c. Hydrology

In this section, we use rainfall and discharge observations to examine the hydrology of flood response in Iowa for the June 2008 storms. Analyses focus on drainage basin water balance analyses of flood response and on scaling of flood peak magnitudes. Hydrologic analyses utilize 15-min Hydro-NEXRAD rain fields. A rain gauge near Decorah was one of the few rain gauges in the area of heaviest rain in Iowa. Daily accumulations for positive rain days during the period 29 May to 13 June from the Decorah rain gauge and Hydro-NEXRAD for the 1-km^2 pixel containing the gauge show excellent agreement (R^2 greater than 0.9; figure not shown), with the 8 June Hydro-NEXRAD accumulations (128 mm) only slightly smaller than the rain gauge accumulation (141 mm). For reference (here and below), the 10-, 50-, 100-, and 500-yr

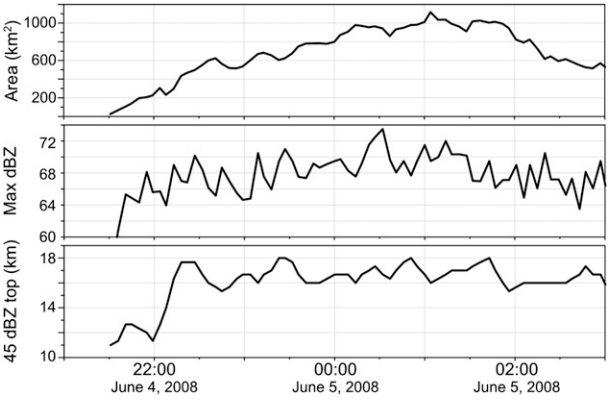

FIG. 11. Time series of storm area, maximum reflectivity, and the 45 dBZ storm height based on Thunderstorm Identification Tracking and Nowcasting (TITAN) storm tracking analyses for the supercell thunderstorm circled in Fig. 7 (top panel).

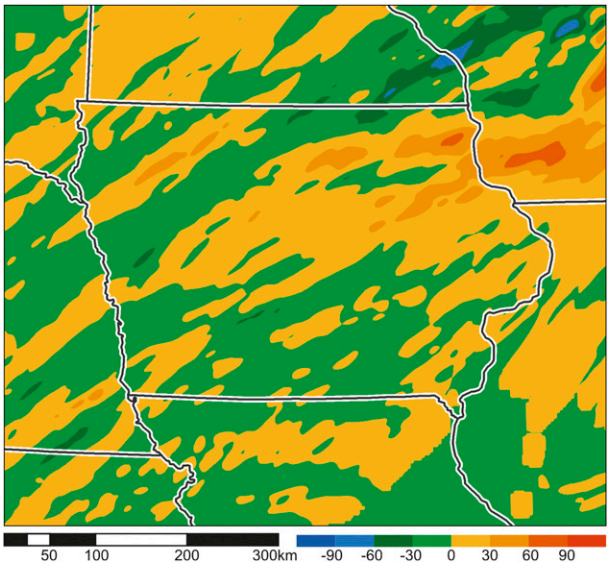

FIG. 12. Spatial map of the difference in WRF simulations of rainfall (mm) for weak coupling ($C = 0.5$) and strong coupling ($C = 0.1$). Details of the simulations are presented in the text.

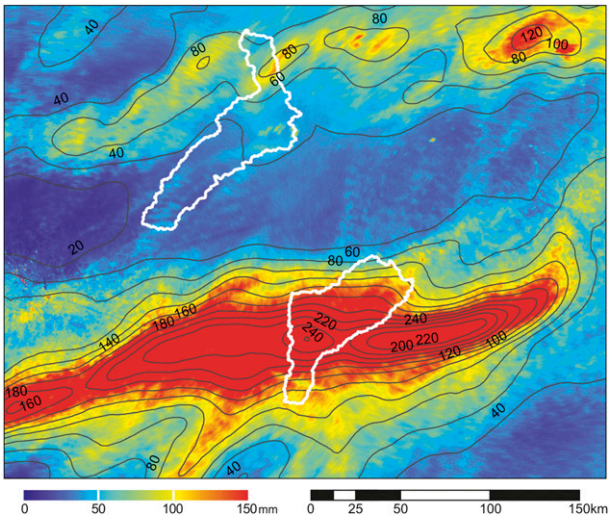

FIG. 13. Total rainfall (mm) from 4 to 6 June 2008 over southwestern Iowa based on Hydro-NEXRAD rainfall fields (see text for details on rainfall analyses and Fig. 1 for geographic setting).

rainfall accumulations for northeastern Iowa are approximately 110, 150, 165, and 210 mm, respectively. For 48 h (see analyses below), the 10-, 50-, 100-, and 500-yr rainfall accumulations are approximately 125, 165, 185, and 230 mm, respectively [based on National Oceanic and Atmospheric Administration (NOAA) precipitation frequency atlas values; http://www.nws.noaa.gov/oh/hdsc/index.html].

Record flooding in the Nodaway River basin (Fig. 6, top) resulted from rainfall on 5–6 June that concentrated over the Nodaway and adjacent basins (Fig. 13). Rainfall in the Nodaway for the 5–6 June storm ranged from 70 mm in the northern portion of the basin to 240 mm in the central portion of the basin to 70 mm in the southern portion of the basin. For the 5–6 June storm, rainfall in the Nodaway was 169 mm, runoff was 87 mm, and the runoff ratio was 51% (see additional discussion below).

Record flooding in northeastern Iowa (Fig. 6, bottom) was produced by rainfall from 1200 UTC 7 June until 1200 UTC 9 June (Fig. 14), which produced a swath of heavy rain that cut through the upper portion of the Cedar River basin, with large south-to-north spatial gradients. In the Shell Rock River basin, rainfall for the period ranged from 40 mm in the upper boundary of the basin in Minnesota to a maximum of 180 mm in the central portion of the Shell Rock to 60 mm at the outlet of the basin. Mean rainfall over the Shell Rock for the period was 118 mm. Catastrophic flooding in the Nodaway, Shell Rock, and lower Cedar River basin did not result from uniform heavy rain over the basin, but from a complex distribution of rainfall reflecting storm structure and evolution.

The Upper Iowa River basin was located in the area of peak rainfall during the 7–9 June period (Fig. 14), with relatively uniform accumulations of 170–180 mm over the basin. The Upper Iowa experienced record flooding at all three stream gauging stations (Fig. 15). Peak discharge values increased from 470 $m^3 s^{-1}$ at 951 km^2 to 965 $m^3 s^{-1}$ at 1323 km^2, but decreased to 883 $m^3 s^{-1}$ at 1994 km^2 (Fig. 15). Temporal variability in rainfall distribution resulted in a sequence of local maxima in the time series of discharge (Fig. 15). The timing of heavy rainfall in the lower portion of the basin resulted in the lower station peaking prior to the upstream station. The peak discharge from the middle station was attenuated, resulting in a second lower peak at the downstream station.

We separated the Upper Iowa River hydrographs from the 7–9 June and 12 June storms (see Fig. 15) by taking the recession for the second event and splicing it onto the first event. Runoff values for the 7–9 June storm were 89, 115, and 103 mm, from rainfall accumulations of 179, 178, and 171 mm, yielding runoff ratios of 50%, 65%, and 69%, respectively. Runoff values for the 12 June storm were 19, 18, and 21 mm from rainfall accumulations of 42, 43, and 43 mm, yielding runoff ratios of 45%, 42%, and 49%, respectively.

Similar analyses were carried out for the five flood events in the Nodaway River basin (Fig. 6). Runoff was estimated for each event, as in the Upper Iowa analyses. For the five events, the sequence of rain and runoff ratios are 40 mm and 33%, 34 mm and 16%, 169 mm and

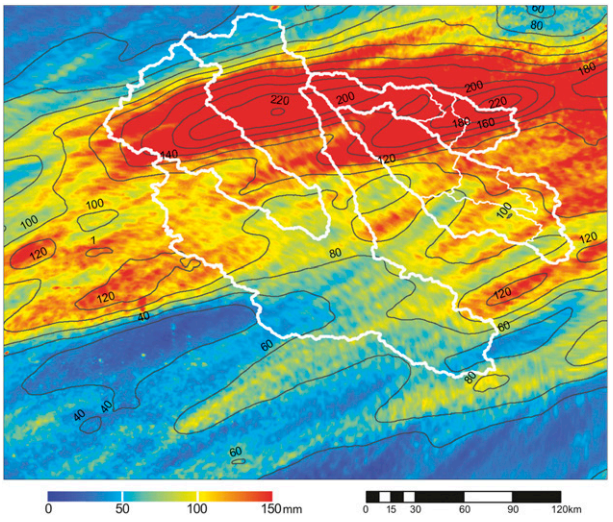

FIG. 14. As in Fig. 13, but from 7 to 9 June 2008 over northeastern Iowa.

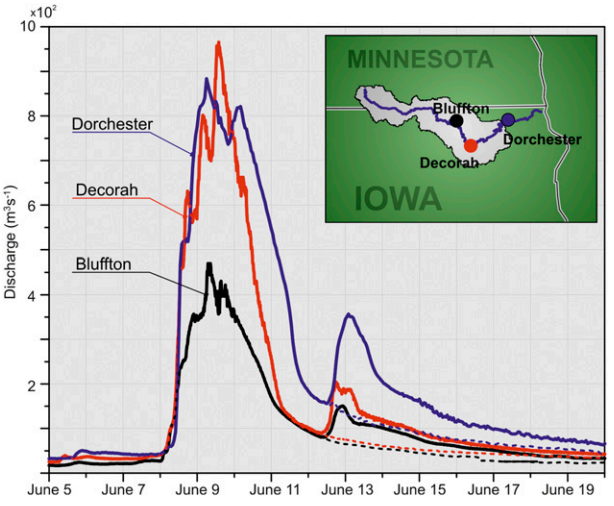

FIG. 15. Discharge time series for the Upper Iowa River at Bluffton (05387440), Decorah (05387500), and Dorchester (05388250) for the period 5–19 June 2008.

51%, 47 mm and 35%, and 90 mm and 44%. Rain minus runoff for the five events yields 26, 28, 84, 31, and 50 mm. Runoff increases with rainfall, but there is little evidence in the Nodaway and Upper Iowa analyses that runoff ratios increased over the sequence of storms because of elevated antecedent moisture. The Nodaway basin is largely agricultural, and as discussed in section 3a, has experienced a significant increase in annual flood peaks during the past 75 years. The role of tile drains in modifying flood response is a major question that emerged from the June 2008 flooding (Mutel 2010); future modeling studies will build on the analyses presented above to examine this question.

For the Turkey River basin, the largest flood peak occurred at the upper Turkey River gauging station at Eldorado (Fig. 16; drainage area of 1660 km^2). The upper Turkey River received the largest rainfall accumulations from the 7–9 June storms (Fig. 14). The discharge hydrograph at the downstream station at Garber (drainage area of 4002 km^2) has two nearly identical peaks separated by 36 h (Fig. 16). The first peak is a combination of contributions from the Volga tributary (drainage area of 901 km^2) and runoff from the main stem basin downstream of Eldorado (reflected in the first and smaller peak at the Elkader gauging station, which has a drainage area of 2339 km^2). The second peak at Garber is principally due to the upstream peak from Eldorado. Rainfall distribution, drainage network structure, and channel/floodplain attenuation of flood waves combine to produce the pattern of peak discharge over the drainage network of the Turkey River (Fig. 16).

The peak discharge of 3964 $m^3 s^{-1}$ for the Cedar River at Cedar Rapids occurred at approximately 1000 Central Daylight Time (CDT) on 13 June (Fig. 17, Table 1; 1000 CDT is midpoint of a 6-h period with constant measured discharge at the 3964 $m^3 s^{-1}$ peak). Flood peaks for the Cedar River at Waverly (1489 $m^3 s^{-1}$ at 4007 km^2), Shell Rock River (1709 $m^3 s^{-1}$ at 4522 km^2), and West Fork Cedar River (733 $m^3 s^{-1}$ at 2191 km^2) on 10 June combined to produce the flood peak of 3170 $m^3 s^{-1}$ for the Cedar River at Waterloo (13 328 km^2) at 0300 CDT on 11 June (Fig. 17, Table 1). The timing of rainfall distribution and flood peak occurrence indicates that flood response for the Cedar River above Waterloo was principally due to rainfall from the 8 June storm. The same is true for the downstream peak at Cedar Rapids 55 h after the Waterloo peak. The travel time of the flood wave from Waterloo to Cedar Rapids is comparable to travel times for major recent floods. The 27 May 2004 flood peak of 1769 $m^3 s^{-1}$ at Cedar Rapids occurred 51 h after the upstream peak of 1656 $m^3 s^{-1}$ at Waterloo. The May 2004 peak is the third-largest peak at Cedar Rapids in the past 40 years (behind the 2008 and 1993 peaks).

There are significant uncertainties in discharge estimates for extreme floods (Potter and Walker 1981), and inconsistencies in discharge estimates for the Cedar River basin (Table 1) are tied to these uncertainties. The magnitude of the Cedar Rapids peak discharge is anomalously large, even in comparison to the record flood peak upstream at Waterloo. Runoff estimates for the Cedar River basin gauging stations were computed for the period 28 May to 30 June. Missing records were reconstructed for the Cedar Rapids station by the USGS, but the reconstruction has relatively little impact on runoff computations because the peak response is well constrained by observations. Runoff for the 34-day

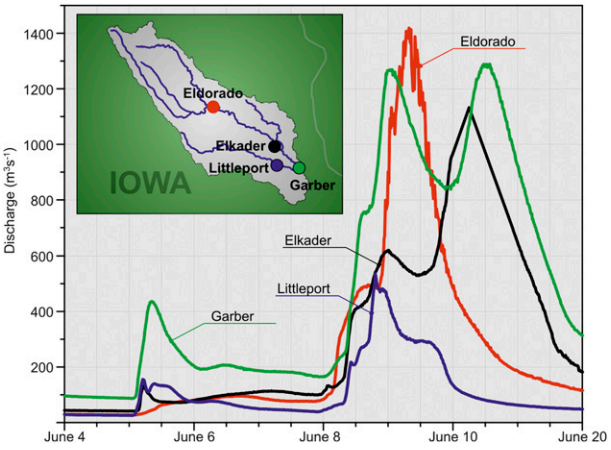

FIG. 16. As in Fig. 15, but for the Turkey River at Eldorado (05411850), Elkader (05412020), Volga River at Littleport (05412400), and Turkey River at Garber (05412500).

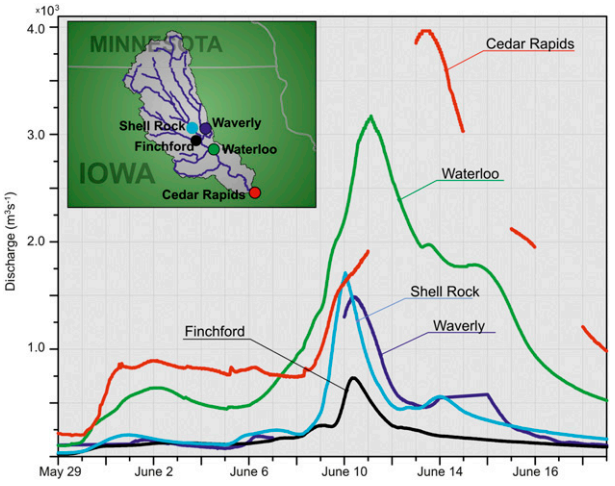

FIG. 17. As in Fig. 15, but for the Cedar River at Cedar Rapids (05464500), Cedar River at Waterloo (05464000), Shell Rock River (05462000), West Fork Cedar River at Finchford (05458900), and Cedar River at Waverly (05458300) for the period 28 May to 21 June 2008.

period was 209 mm for the Cedar Rapids station and 191 mm for the Waterloo station. This implies that the runoff for the intervening drainage area (3533 km^2) was 280 mm. Rainfall in the intervening area, however, was much lower than in upstream portions of the basin (see, for example, the key rain period in Fig. 14 and Table 2). The 191-mm runoff from the Waterloo station is larger than the runoff values from Shell Rock (168 mm), Cedar River at Waverly (172 mm), and West Fork Cedar River basin (186 mm). The drainage area of these three stations accounts for almost 80% of the drainage basin above Waterloo. These observations suggest that the estimated Cedar River flood peak at Cedar Rapids may be too high.

The June 2008 flood peaks over the Cedar–Iowa River system (Fig. 18, Table 2) exhibit a pronounced log–log linear relationship between drainage area and peak discharge (see Gupta et al. 2010). Embedded in the log–log linear relationship are important details linking rainfall variability, channel/floodplain attenuation of flood waves, and river regulation to scale-dependent flood response (as well as the measurement issues raised above for peak discharge estimates). The spatial distribution of rainfall (see, e.g., Fig. 14) plays a key role in storm event scaling analyses of flood peaks. The relatively large peak in Beaver Creek (28 in Fig. 18) and the relatively small peak in Old Man's Creek (17) simply reflect contrasting rainfall distribution, with lower rainfall accumulations in Old Man's Creek resulting in smaller peaks and peak rainfall in Beaver Creek resulting in anomalously large flood peaks relative to the regional scaling relationship.

The scaling properties for the Iowa River include significant impacts from dams. The downstream sequence of stations in the Iowa River exhibits a sharp decrease from Marengo (10) to Coralville (11) associated with the Coralville Dam. There is a slight increase from Coralville to Iowa City (16), and the peak for the downstream gauge at Lone Tree (19) exceeds the upstream gauge at Margeno (10). The lower Cedar River stations show the sharp increase from Waterloo (30) to Cedar Rapids (33) and then a sharp decrease to Conesville (34), which reflects channel–floodplain attenuation of peak discharge as well as potential errors in peak discharge estimation as discussed above. The combined Cedar–Iowa River peak of the Iowa River at Wapello (35) reflects an additive combination of the Cedar River at Conesville (34) and the Iowa River at Lone Tree (19). In examining scaling properties of flood peaks, it is also important to consider uncertainties in flood peak estimates for extreme floods, as discussed above.

The log–log linear relationship for the June 2008 flooding is not as clearly reflected in recent major floods in the Cedar–Iowa River system (Fig. 19). The scaling analyses for July 1993 (Fig. 19, top) reflect rainfall maxima in the Iowa River basin, while the May 2004 analyses (Fig. 19, bottom) reflect rainfall maxima in the eastern Cedar River basin. Exponents in the power law scaling relationships take the values 0.69 for the 1993 flood, 0.89 for the 2004 flood, and 0.78 for the June 2008 flood [compare with analyses in Ogden and Dawdy (2003) for the Goodwin Creek Experimental Watershed in which exponents average 0.82]. One of the anomalous features of the June 2008 flood (see section 3a) was the spatial extent of flooding. The only historical flood that compared with the June 2008 flood was the 1993 flood. Scaling analyses of flood peaks (Figs. 18, 19) point to the complexity of extreme floods, but they also focus attention

TABLE 1. Flood summary for the Cedar River basin.

Name	USGS ID	Area (km^2)	Peak ($m^3 s^{-1}$)	Time	Runoff (mm)	Rainfall (mm)
Cedar R. at Waverly	05458300	4007	1489	10 June	172	409
Cedar R. at Janesville	05458500	4302	1511	10 June	189	405
Shell Rock	05462000	4522	1709	10 June	168	370
West Fork Cedar	05458900	2191	733	10 June	186	346
Cedar R. at Waterloo	05464000	13328	3170	11 June	191	378
Cedar R. at Cedar Rapids	05464500	16861	3962	13 June	209	370

on the spatial distribution of extreme rainfall as the lead actor in controlling flood peak scaling in regions for which warm season convective systems are the principal flood agents.

4. Summary and conclusions

The hydroclimatology, hydrometeorology, and hydrology of extreme flooding are examined through analyses of rainfall, runoff, and flood peak magnitudes for the June 2008 flood event in Iowa. Analyses of the June 2008 flood are placed in a climatological context based on long discharge records in the region. Analyses are designed to provide insights into the key mechanisms associated with the frequency and magnitude of extreme floods in regions for which organized thunderstorm systems are major flood agents. The major findings of this paper are as follows.

TABLE 2. Flood peak summary for scaling analyses.

No.	Name	USGS ID	Area (km^2)	Peak ($m^3 s^{-1}$)
1	Iowa R. near Rowan	05449500	1111	223
2	S. Fork Iowa R. near Blairsburg	05451080	31	22
3	S. Fork Iowa R. northeast of New Providence	05451210	580	209
4	Iowa R. at Marshalltown	05451500	3968	634
5	Timber Creek near Marshalltown	05451700	306	199
6	Richland Creek	05451900	145	70
7	Salt Creek	05452000	521	354
8	Walnut Creek	05452200	184	133
9	Big Bear Creek	05453000	490	190
10	Iowa R. at Marengo	05453100	7236	1444
11	Iowa R. below Coralville	05453520	8068	1124
12	Rapid Creek	05454000	66	20
13	Muddy Creek	05454090	23	27
14	Clear Creek near Oxford	05454220	151	62
15	Clear Creek near Coralville	05454300	254	80
16	Iowa R. at Iowa City	05454500	8471	1147
17	Old Man's Creek	05455100	521	97
18	English River	05455500	1487	261
19	Iowa R. near Lone Tree	05455700	11 119	1506
20	Cedar R. near Austin, MN	05457000	1033	433
21	Cedar R. at Charles City	05457700	2730	614
22	Little Cedar R.	05458000	793	467
23	Cedar R. at Waverly	05458300	4007	1489
24	Cedar R. at Janesville	05458500	4302	1511
25	W. Fork Cedar R.	05458900	2191	733
26	Winnebago R.	05459500	1362	371
27	Shell Rock R.	05462000	4522	1709
28	Beaver Creek	05463000	899	733
29	Black Hawk Creek	05463500	785	334
30	Cedar R. at Waterloo	05464000	13 328	3170
31	Wolf Creek	05464220	774	268
32	Cedar R. at Cedar Rapids	05464500	16 861	3964
33	Hoover Creek	05464942	7.8	7.7
34	Cedar R. near Conesville	05465000	20 168	3596
35	Iowa R. at Wapello	05465500	32 375	5324

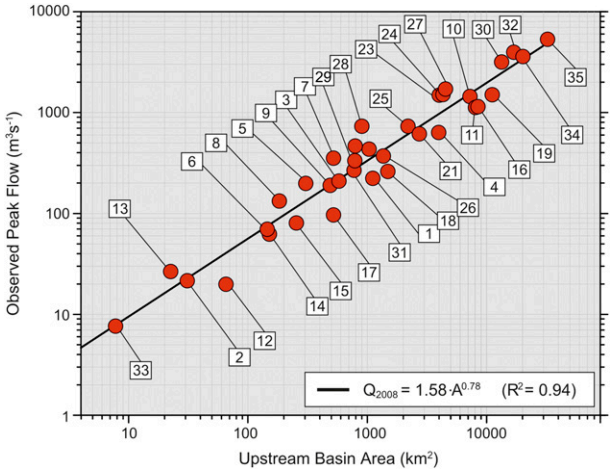

FIG. 18. Log–log scaling of flood peaks for the June 2008 floods in Iowa. See Table 2 for relation between numbers and USGS stream gauging stations.

- Extreme flooding occurred in the Cedar River basin during June 2008, with the Cedar River at Cedar Rapids (drainage area of 16 861 km^2) experiencing a record flood peak of 3965 m^3 s^{-1} that was nearly twice as large as the second-largest peak from a record of more than 100 years. GEV analyses of annual flood peak data indicate that the return interval for the Cedar Rapids peak is longer than 300 years. Record flooding occurred throughout large segments of Iowa with 10 out of 41 nonnested basins in Iowa with long flood records (more than 50 years) experiencing record flooding. The most important caveats concerning analyses of flood frequency for the June 2008 floods concern measurement error. There are significant uncertainties in estimated peak discharge values in the Cedar River basin for the June 2008 flood, as is typically the case for extreme floods (Potter and Walker 1981). Runoff and rainfall analyses for the Cedar River basin suggest that the Cedar Rapids peak may be too high.
- Analyses of peaks-over-threshold flood peaks suggest that clustering is an important feature of the flood occurrence process in Iowa. The June 2008 flooding in Iowa was associated with a series of rain events that occurred from 30 May through 14 June. Clustering is potentially important over a range of time scales, extending from the multiple-day occurrence of heavy rainfall events to dependence over the entire warm season (Villarini et al. 2013). Future studies should assess the relative importance of atmospheric processes and land surface processes in controlling clustering of flood occurrences, both for the entire population of floods and for extreme floods.
- The storms that produced record flooding in southwestern Iowa during the 5–6 June period were severe thunderstorm systems that produced multiple tornados. Similarly, the 7–8 June storms included severe thunderstorm systems with tornados and damaging winds. Analyses of the June 2008 storm systems support previous observations that severe thunderstorm systems, including supercell thunderstorms, are important agents in determining the upper tail of flood peaks in the United States east of the Rocky Mountains (Smith et al. 2001). The period of flooding during

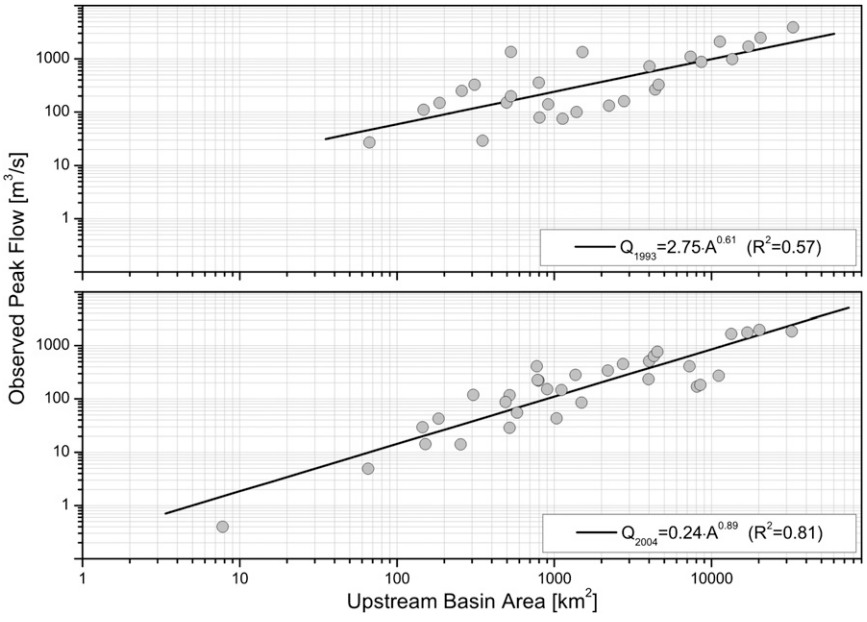

FIG. 19. Log–log scaling of flood peaks for the (top) 1993 and (bottom) 2004 floods in Iowa.

June 2008 coincides with a sharp seasonal maximum in flood occurrence for Iowa. Spatial variation in seasonality of flood frequency is pronounced over the study region and reflects the climatology of mesoscale convective systems (Schumacher and Johnson 2006).

- Heavy rainfall during June 2008 was associated with periods of strong atmospheric water vapor convergence. The June 2008 storm systems, like many other flood-producing storm systems in the region, were associated with a warm season extratropical cyclone and large moisture transport from the Gulf of Mexico associated with westward displacement of the Bermuda high. Simulations of the June 2008 storm systems over Iowa with WRF were carried out to examine sensitivity of heavy rainfall to land surface processes. These analyses suggest that land surface processes may alter the details of rainfall distribution, but they do not play a major role in determining the occurrence of a major rain event in the region.
- Hydrologic analyses of rainfall and discharge support the hypothesis (see Wood et al. 1990) that the importance of antecedent rainfall for flood peak magnitudes diminishes with return interval. High-resolution radar rainfall fields from Hydro-NEXRAD play an important role in analyses of the role of antecedent rainfall on flood response for the June 2008 storms.
- Flood peak magnitudes in the Cedar–Iowa River basin exhibit pronounced log–log scaling with drainage area (Gupta et al. 2010) for the June 2008 flood event. We show that scaling properties of flood magnitudes for the June 2008 flooding in Iowa are linked to the spatial and temporal distribution of rainfall, drainage network structure, flood peak attenuation, and river regulation by dams. Scaling analyses for major flood events in June 1993 and May 2004 highlight the central role of rainfall distribution for flood peak scaling. Uncertainties in peak discharge estimates, as summarized above, also play an important role in characterizations of flood peak scaling based on observations from stream gauging stations.

Acknowledgments. This research was supported by the National Science Foundation (NSF Grant EAR-0847347), NASA (Grant NNX10AI46G), the NOAA Cooperative Institute for Climate Science (CICS), the Iowa Flood Center, and the Willis Research Network. We would also like to acknowledge the assistance of Radoslaw Goska in preparation of the figures.

REFERENCES

Baeck, M. L., and J. A. Smith, 1998: Rainfall estimation by the WSR-88D for heavy rainfall events. *Wea. Forecasting,* **13,** 416–436.

Borga, M., P. Boscolo, F. Zanon, and M. Sangati, 2007: Hydrometeorological analysis of the 29 August 2003 flash flood in the eastern Italian Alps. *J. Hydrometeor.,* **8,** 1049–1067.

Budikova, D., J. S. M. Coleman, S. A. Strope, and A. Austin, 2010: Hydroclimatology of the 2008 Midwest floods. *Water Resour. Res.,* **46,** W12524, doi:10.1029/2010WR009206.

Carbone, R. E., and J. D. Tuttle, 2008: Rainfall occurrence in the U.S. warm season: The diurnal cycle. *J. Climate,* **21,** 4132–4146.

Changnon, S. A., and K. E. Kunkel, 1995: Climate-related fluctuation in Midwestern floods during 1921–1985. *J. Water Resour. Plann. Manage.,* **121,** 326–334.

Coleman, J. S. M., and D. Budikova, 2010: Atmospheric aspects of the 2008 Midwest floods: A repeat of 1993? *Int. J. Climatol.,* **30,** 1645–1667.

Coles, S., 2001: *An Introduction to Statistical Modeling of Extreme Values.* Springer, 208 pp.

Cotton, W. L., and R. Anthes, 1989: *Storm and Cloud Dynamics.* Academic Press, 883 pp.

DeAngelis, A., F. Dominguez, Y. Fan, A. Robock, M. Deniz Kustu, and D. Robinson, 2010: Evidence of enhanced precipitation due to irrigation over the Great Plains of the United States. *J. Geophys. Res.,* **115,** D15115, doi:10.1029/2010JD013892.

Dirmeyer, P. A., and K. L. Brubaker, 1999: Contrasting evaporative moisture sources during the drought of 1988 and the flood of 1993. *J. Geophys. Res.,* **104** (D16), 19 383–19 397.

Dixon, M., and G. Wiener, 1993: TITAN: Thunderstorm Identification, Tracking, Analysis, and Nowcasting—A radar-based methodology. *J. Atmos. Oceanic Technol.,* **10,** 785–797.

Doswell, C. A., H. E. Brooks, and R. A. Maddox, 1996: Flash flood forecasting: An ingredients-based methodology. *Wea. Forecasting,* **11,** 560–581.

Fulton, R., J. P. Breidenbach, D. J. Seo, D. A. Miller, and T. O'Bannon, 1998: The WSR-88D rainfall algorithm. *Wea. Forecasting,* **13,** 377–398.

Georgakakos, K. P., and D. H. Bae, 1994: Climatic variability of soil-water in the American Midwest: Part 2. Spatiotemporal analysis. *J. Hydrol.,* **162,** 379–390, doi:10.1016/0022-1694(94)90237-2.

Guetter, A. K., and K. P. Georgakakos, 1996: Are the El Niño and La Niña predictors of the Iowa River seasonal flow? *J. Appl. Meteor.,* **35,** 690–705.

Gupta, V. K., R. Mantilla, B. M. Troutman, D. Dawdy, and W. F. Krajewski, 2010: Generalizing a nonlinear geophysical flood theory to medium-sized river networks. *Geophys. Res. Lett.,* **37,** L11402, doi:10.1029/2009GL041540.

Krajewski, W. F., G. Villarini, and J. A. Smith, 2010a: Radar-rainfall uncertainties: Where are we after thirty years of effort? *Bull. Amer. Meteor. Soc.,* **91,** 87–94.

——, and Coauthors, 2010b: Towards better utilization of NEXRAD data in hydrology: An overview of Hydro-NEXRAD. *J. Hydroinf.,* **13,** 255–266, doi:10.2166/hydro.2010.056.

Kunkel, K. E., S. A. Changnon, and J. R. Angel, 1994: Climatic aspects of the 1993 Upper Mississippi River basin flood. *Bull. Amer. Meteor. Soc.,* **75,** 811–822.

Kustu, M. D., Y. Fan, and M. Rodell, 2011: Possible link between irrigation in the US High Plains and increased summer streamflow in the Midwest. *Water Resour. Res.,* **47,** W03522, doi:10.1029/2010WR010046.

LeMone, M. A., M. Tewari, F. Chen, J. G. Alfieri, and D. Niyogi, 2008: Evaluation of the Noah land surface model using data from a fair-weather IHOP_2002 day with heterogeneous surface fluxes. *Mon. Wea. Rev.,* **136,** 4915–4941.

Lin, N., J. A. Smith, G. Villarini, T. P. Marchok, and M. L. Baeck, 2010: Modeling extreme rainfall, winds, and surge from Hurricane Isabel (2003). *Wea. Forecasting,* **25,** 1342–1361.

McAnelly, R. L., and W. R. Cotton, 1989: The precipitation life cycle of mesoscale convective complexes over the central United States. *Mon. Wea. Rev.,* **117,** 784–808.

Merz, R., and G. Blöschl, 2003: A process typology of regional floods. *Water Resour. Res.,* **39,** 1340, doi:10.1029/2002WR001952.

Morin, E., D. C. Goodrich, R. A. Maddox, X. G. Gao, H. V. Gupta, and S. Sorooshian, 2006: Spatial patterns in thunderstorm rainfall events and their coupling with watershed hydrological response. *Adv. Water Resour.,* **29,** 843–860, doi:10.1016/j.advwatres.2005.07.014.

Mutel, C., 2010: *A Watershed Year: Anatomy of the Iowa Floods of 2008*. University of Iowa Press, 284 pp.

Ntelekos, A. A., J. A. Smith, M. L. Baeck, W. F. Krajewski, A. J. Miller, and R. Goska, 2008: Extreme hydrometeorological events and the urban environment: Dissecting the 7 July 2004 thunderstorm over the Baltimore, MD, metropolitan region. *Water Resour. Res.,* **44,** W08446, doi:10.1029/2007WR006346.

Ogden, F. L., and D. W. Dawdy, 2003: Peak discharge scaling in small hortonian watersheds. *J. Hydrol. Eng.,* **8,** 64–73.

Paegle, J., K. C. Mo, and J. N. Paegle, 1996: Dependence of simulated precipitation on surface evaporation during the 1993 United States summer floods. *Mon. Wea. Rev.,* **124,** 345–361.

Potter, K. W., 1991: Hydrological impacts of changing land management practices in a moderate-sized agricultural catchment. *Water Resour. Res.,* **27,** 845–855.

——, and J. F. Walker, 1981: A model of discontinuous measurement error and its effects on the probability distribution of flood discharge measurements. *Water Resour. Res.,* **17,** 1505–1509.

Rasmusson, E. M., 1967: Atmospheric water vapor transport and water balance of North America: Part I. Characteristics of the water vapor flux field. *Mon. Wea. Rev.,* **95,** 403–426.

Reed, S. M., and D. R. Maidment, 1999: Coordinate transformation for using NEXRAD data in GIS-based hydrologic modeling. *J. Hydrol. Eng.,* **4,** 174–182.

Robinson, J. S., M. Sivapalan, and J. D. Snell, 1995: On the relative roles of hillslope processes, channel routing, and network geomorphology in the hydrologic response of natural catchments. *Water Resour. Res.,* **31,** 3089–3101.

Saco, P. M., and P. Kumar, 2002: Kinematic dispersion in stream networks: 1. Coupling hydraulic and network geometry. *Water Resour. Res.,* **38,** 1244, doi:10.1029/2001WR000695.

Schilling, K. E., and R. D. Libra, 2003: Increased baseflow in Iowa over the second half of the 20th century. *J. Amer. Water Resour. Assoc.,* **39,** 851–860.

——, M. K. Jha, Y. K. Zhang, P. W. Gassman, and C. F. Wolter, 2008: Impact of land use and land cover change on the water balance of a large agricultural watershed: Historical effects and future directions. *Water Resour. Res.,* **44,** W00A09, doi:10.1029/2007WR006644.

Schumacher, R. S., and R. H. Johnson, 2005: Organization and environmental properties of extreme-rain-producing mesoscale convective systems. *Mon. Wea. Rev.,* **133,** 961–976.

——, and ——, 2006: Characteristics of U.S. extreme rain events during 1999–2003. *Wea. Forecasting,* **21,** 69–85.

Seo, B. C., W. F. Krajewski, A. Kruger, P. Domaszczynski, J. A. Smith, and M. Steiner, 2010: Radar-rainfall estimation algorithms of Hydro-NEXRAD. *J. Hydroinf.,* **13,** 277–291.

Skamarock, W. C., J. B. Klemp, J. Dudhia, D. O. Gill, D. M. Barker, W. Wang, and J. G. Powers, 2007: A description of the Advanced Research WRF version 2. NCAR Tech. Note 468+STR, 88 pp. [Available online at http://www.mmm.ucar.edu/wrf/users/docs/arw_v2.pdf.]

Smith, J. A., 1987: Estimating the upper tail of flood frequency distributions. *Water Resour. Res.,* **23,** 1657–1666.

——, 1989: Regional flood frequency analysis using extreme order statistics of the annual peak record. *Water Resour. Res.,* **25,** 311–317.

——, and A. F. Karr, 1986: Flood frequency analysis using the Cox regression model. *Water Resour. Res.,* **22,** 890–896.

——, M. L. Baeck, Y. Zhang, and C. A. Doswell III, 2001: Extreme rainfall and flooding from supercell thunderstorms. *J. Hydrometeor.,* **2,** 469–489.

——, ——, J. E. Morrison, P. Sturdevant-Rees, D. F. Turner-Gillespie, and P. D. Bates, 2002: The regional hydrology of extreme floods in an urbanizing drainage basin. *J. Hydrometeor.,* **3,** 267–282.

——, ——, K. L. Meierdiercks, P. A. Nelson, A. J. Miller, and E. J. Holland, 2005: Field studies of the storm event hydrologic response in an urbanizing watershed. *Water Resour. Res.,* **41,** W10413, doi:10.1029/2004WR003712.

——, ——, A. A. Ntelekos, G. Villarini, and M. Steiner, 2011: Extreme rainfall and flooding from orographic thunderstorms in the central Appalachians. *Water Resour. Res.,* **47,** W04514, doi:10.1029/2010WR010190.

Steiner, M., and J. A. Smith, 2002: Use of three-dimensional structure for automated detection and removal of nonprecipitating echoes in radar data. *J. Atmos. Oceanic Technol.,* **19,** 673–686.

Trier, S. B., F. Chen, K. W. Manning, M. A. LeMone, and C. A. Davis, 2008: Sensitivity of the PBL and precipitation in 12-day simulations of warm-season convection using different land surface models and soil wetness conditions. *Mon. Wea. Rev.,* **136,** 2321–2343.

Tuttle, J. D., and C. A. Davis, 2006: Corridors of warm season precipitation in the central United States. *Mon. Wea. Rev.,* **134,** 2297–2317.

Viglione, A., G. B. Chirico, R. Woods, and G. Bloschl, 2010: Generalised synthesis of space–time variability in flood response: An analytical framework. *J. Hydrol.,* **394,** 198–212, doi:10.1016/j.jhydrol.2010.05.047.

Villarini, G., and J. A. Smith, 2010: Flood peak distributions for the eastern United States. *Water Resour. Res.,* **46,** W06504, doi:10.1029/2009WR008395.

——, F. Serinaldi, and W. F. Krajewski, 2008: Modeling radar-rainfall estimation uncertainties using parametric and nonparametric approaches. *Adv. Water Resour.,* **31,** 1674–1686.

——, J. A. Smith, M. L. Baeck, and W. F. Krajewski, 2011a: Examining flood frequency distributions in the Midwest U.S. *J. Amer. Water Resour. Assoc.,* **43,** 447–463.

——, ——, ——, R. Vitolo, D. B. Stephenson, and W. Krajewski, 2011b: On the frequency of heavy rainfall for the Midwest of the United States. *J. Hydrol.,* **400,** 103–120.

——, ——, R. Vitolo, and D. Stephenson, 2013: On the temporal clustering of US floods and its relationship to climate teleconnection patterns. *Int. J. Climatol.,* **33,** 629–640.

Wang, S. Y., and T. C. Chen, 2009: The late-spring maximum rainfall over the U.S. Central Plains and the role of the low-level jet. *J. Climate,* **22,** 4696–4709.

Wood, E. F., M. Sivapalan, and K. Beven, 1990: Similarity and scale in catchment storm response. *Rev. Geophys.,* **28,** 1–18.

Woods, R., and M. Sivapalan, 1999: A synthesis of space-time variability in storm response: Rainfall, runoff generation, and routing. *Water Resour. Res.,* **35,** 2469–2485.

Zhang, Y., J. A. Smith, and M. L. Baeck, 2001: The hydrology and hydrometeorology of extreme floods in the Great Plains of eastern Nebraska. *Adv. Water Resour.,* **24,** 1037–1049.